Available online at www.sciencedirect.com
ScienceDirect
Optical Materials 29 (2006) 326–331
OPTICAL Materials
www.elsevier.com/locate/optmat

Depth-resolved nanostructure and refractive index of borosilicate glass doped with Ag nanocrystals

H. Mertens *, A. Polman

Center for Nanophotonics, FOM Institute for Atomic and Molecular Physics, Kruislaan 407, 1098 SJ Amsterdam, The Netherlands

Received 26 August 2005; accepted 5 November 2005
Available online 20 December 2005

Abstract

We present an investigation of the Ag-nanocrystal depth profile as well as the corresponding refractive index depth profile of borosilicate glass that was first doped with Ag by $Na^+ \leftrightarrow Ag^+$ ion exchange and subsequently irradiated with 1 MeV Xe ions. By combining RBS, XPS, XE-AES, and transmission and reflection spectroscopy, we show unambiguously that the Ag nanocrystals are formed in a layer with a thickness (90 ± 20 nm) that is significantly smaller than the 1-MeV Xe range (340 nm). The effective refractive index for the highest Xe fluence is $n = 2.1 + 0.8\,i$ at the resonance wavelength ($\lambda = 430$ nm). The implications for the integration of surface-plasmon-resonance-based functionalities in photonic devices based on the described fabrication method are discussed.

PACS: 42.70.Nq; 61.80.Jh; 42.79.Gn

Keywords: Nonlinear optical materials; Ion irradiation; Waveguides

1. Introduction

Composite materials consisting of nobel-metal nanoparticles embedded in a dielectric are known to exhibit surface plasmon resonances (SPR) at optical frequencies [1]. The local electromagnetic field enhancements associated with these resonances enable a broad range of applications including optical switches [2], optical filters [3], bistable devices [4], selective solar absorbers [5], and broadband waveguide polarizers [6].

During the last decades, many experimental methods have been introduced to fabricate such metal–dielectric composites (often referred to as nanocermets). These methods include ion implantation [7], sol–gel processing [8], and sputtering or co-deposition techniques [9]. Also another method, involving a sequence of $Na^+ \leftrightarrow Ag^+$ ion exchange and ion irradiation of Na^+-containing glass, has been proposed [10]. This two-step process enables the fabrication of planar optical waveguides in which Ag nanocrystals are formed in lithography-defined sections, since mask-assisted ion irradiation can be applied to locally nucleate Ag nanocrystals [11]. Consequently, this approach provides the possibility of integrating SPR-based functionalities in photonic devices. As an example, Fig. 1 shows a schematic of a planar waveguide in which nanocrystal-doped regions are formed in order to fabricate a nonlinear Bragg grating. Two-dimensional nonlinear photonic crystals have also been proposed [11]. Crucial for these applications is the local control of nanocrystal formation by ion irradiation.

In order to form well-defined Ag-nanoparticle sections with controlled optical properties, a detailed knowledge of the ion-beam-induced changes of material properties is of crucial importance. With that in mind, we present an investigation of the Ag-nanocrystal depth profile as well as the corresponding refractive index depth profile of $Na^+ \leftrightarrow Ag^+$ ion-exchanged and subsequently Xe-irradiated borosilicate glass. The analysis is based on Rutherford backscattering spectrometry (RBS), X-ray photoelectron spectroscopy

* Corresponding author. Tel.: +31 20 608 1234; fax: +31 20 668 4106.
E-mail address: mertens@amolf.nl (H. Mertens).

0925-3467/$ - see front matter
doi:10.1016/j.optmat.2005.11.002

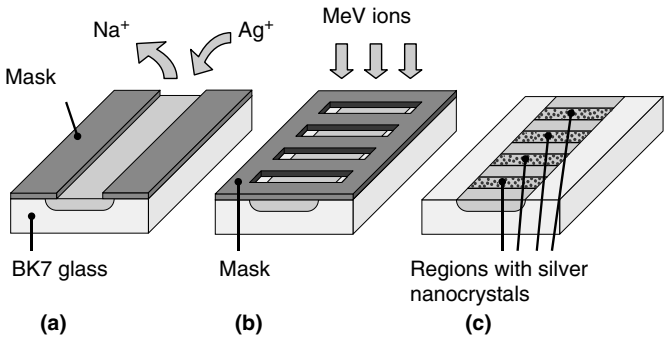

Fig. 1. Schematic illustration of the fabrication process of a planar waveguide with nanocrystal-doped regions: (a) waveguide definition by a standard $Na^+ \leftrightarrow Ag^+$ ion-exchange process, (b) nanocrystal formation by MeV ion irradiation using a mask-assisted process, and (c) the resulting metallodielectric Bragg grating.

(XPS), X-ray-excited Auger spectroscopy (XE-AES), and optical transmittance and reflectance measurements. We conclude that the Ag nanocrystals are formed in a layer with a thickness that is significantly smaller than the range of the ions used to induce the nucleation, and we derive the optical constants for the Ag-nanocrystal-doped layer.

2. Experimental

Ag nanocrystals were formed in Na^+-containing Schott BK7 glass by a combination of $Na^+ \leftrightarrow Ag^+$ ion exchange and 1 MeV Xe ion irradiation. The composition of the BK7 glass before ion exchange was 23 at.% Si, 61 at.% O, 5 at.% B, 7 at.% Na, 3 at.% K, 0.2 at.% Ba, as was determined by Rutherford backscattering spectrometry (RBS). Samples of 1 mm thickness were ion-exchanged at 350 °C for 10 min in a salt melt of 5 mol% $AgNO_3$ in $NaNO_3$. Subsequently, Ag nanocrystals were formed by 1 MeV Xe irradiation (ion range: 340 nm) under normal incidence at 77 K. Three samples were exposed to different fluences: 5.5×10^{14}, 3.0×10^{15}, and 1.0×10^{16} ions/cm^2, respectively. Transmission electron microscopy (TEM) has shown that this leads to the formation of Ag nanoparticles with diameters ranging from below 3.5 nm to 10–15 nm [12].

RBS was performed using a 2 MeV He beam to determine the Ag depth profile of the $Na^+ \leftrightarrow Ag^+$ ion-exchanged borosilicate glass before and after Xe irradiation. In addition, X-ray photoelectron spectroscopy (XPS) and X-ray excited Auger spectroscopy (XE-AES) were performed to identify the Ag chemical state as function of depth (range 10–450 nm) [13,14]. These measurements were done with a PHI Quantera scanning X-ray microprobe, using 1 keV Ar sputtering for depth profiling (accuracy: ±10%). Optical transmittance and specular reflectance were measured at (near-)normal incidence in the spectral range of 1.2–4 eV (1000–300 nm), using a variable-angle spectroscopic ellipsometer. Simulations, based on the transfer matrix method and the Maxwell–Garnett effective medium theory, were performed to model the depth-dependent optical constants.

3. Results and discussion

3.1. Ag depth profile

Fig. 2 shows the Ag depth profile of unirradiated and 1 MeV Xe irradiated $Na^+ \leftrightarrow Ag^+$ ion-exchanged borosilicate glass as obtained by RBS. Both Ag^0 and Ag^+ are represented in Fig. 2, as RBS is insensitive to the Ag chemical state. The unirradiated sample, having an Ag concentration of 7 at.% at the surface, shows a gradual decrease in Ag concentration as a function of depth, which is typical for the ion exchange process. The depth profile of the 1 MeV Xe irradiated sample (fluence: 1.0×10^{16} ions/cm^2) shows Ag accumulation in a layer of ~80 nm directly below the surface (Ag peak concentration 9 at.%) and Ag depletion underneath that layer extending to a depth of >800 nm. The depth profiles of the samples irradiated at the other fluences exhibit a similar trend (not shown).

Ag accumulation in a layer directly below the surface and Ag depletion beneath that layer has also been observed in Ag-containing borosilicate glass that was thermally annealed in hydrogen [15]. This effect has been attributed to Ag reduction in the surface region and subsequent Ag^+ migration towards the surface due to the reduction-induced change in the Ag^+ electrochemical potential [16]. Accordingly, the Ag depth profiles shown in Fig. 2 would indicate that Ag nanoparticles (Ag^0) are mainly present in the first ~80 nm below the surface.

3.2. Ag^0 depth profile

Fig. 3 shows the XE-AES spectra of (a) unirradiated and (b) 1 MeV Xe irradiated (fluence: 1.0×10^{16} ions/cm^2) $Na^+ \leftrightarrow Ag^+$ ion-exchanged borosilicate glass at depths between 10 and 200 nm. The energy range is such that the Ag $M_4N_{45}N_{45}$ (358 eV) and $M_5N_{45}N_{45}$ (352 eV) Auger

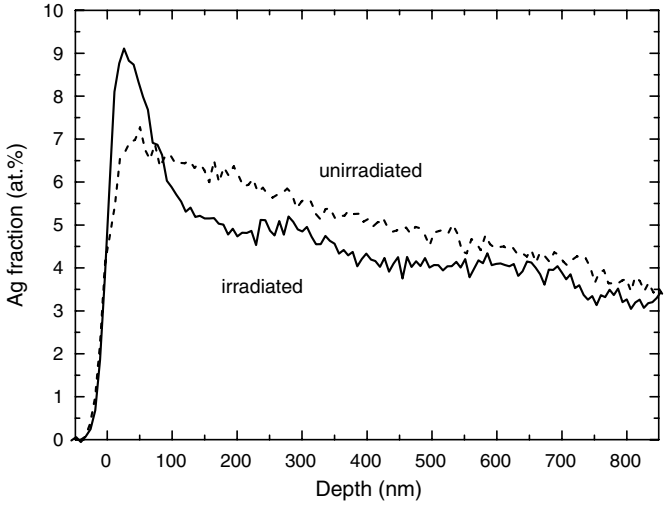

Fig. 2. Ag depth profile, obtained by RBS, of unirradiated (dashed line) and 1 MeV Xe irradiated (solid line) $Na^+ \leftrightarrow Ag^+$ ion-exchanged borosilicate glass. The Xe fluence for the irradiated sample is 1.0×10^{16} ions/cm^2.

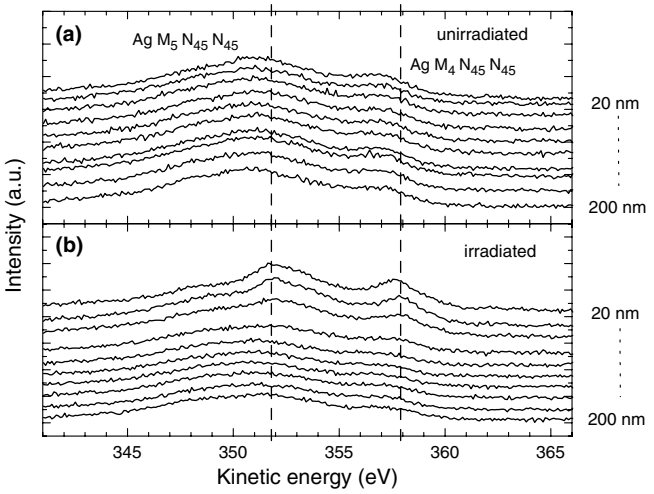

Fig. 3. XE-AES spectra of the Ag $M_4N_{45}N_{45}$ and $M_5N_{45}N_{45}$ Auger lines of (a) unirradiated and (b) 1 MeV Xe irradiated (fluence: 1.0×10^{16} ions/cm^2) $Na^+ \leftrightarrow Ag^+$ ion-exchanged borosilicate glass over a depth range of 20–200 nm (with a 20-nm step size). The spectra are shifted vertically for clarity. The dashed vertical lines indicate the peak positions for the Ag^0 chemical state.

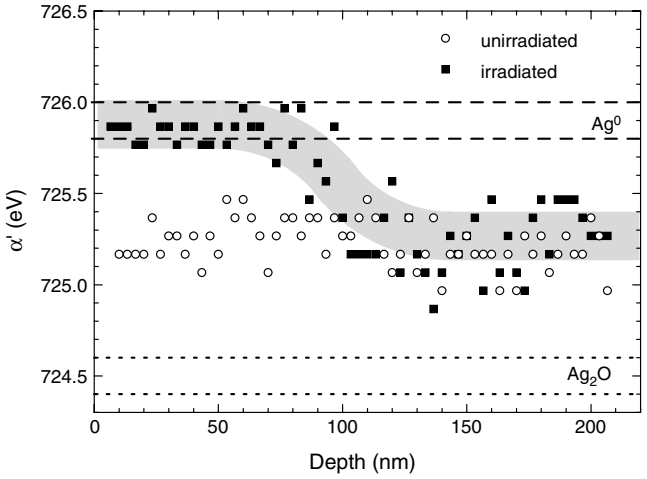

Fig. 4. Modified Auger parameter α' for Ag as function of depth, obtained by XPS and XE-AES, over a depth range of 20–200 nm (with a 3-nm step size), for unirradiated (○) and 1 MeV Xe irradiated (■) $Na^+ \leftrightarrow Ag^+$ ion-exchanged borosilicate glass. The Xe fluence for the irradiated sample is 1.0×10^{16} ions/cm^2. The gray band is a guide to the eye representing the trend for the irradiated sample. The literature values for Ag^0 and Ag_2O are indicated for reference.

lines are visible; both are sensitive to the Ag chemical state. The spectra obtained from the unirradiated sample all look similar, and the peak positions are fairly constant over depth. In contrast, the spectra obtained from the irradiated sample show a clear shift in Ag $M_4N_{45}N_{45}$ and $M_5N_{45}N_{45}$ Auger lines for the first 60–100 nm. In fact, the corresponding peak positions are found to coincide with the peak energies for Ag^0 measured on a pure-Ag reference sample, which are indicated as dashed vertical lines in Fig. 3. Hence, XE-AES proves that only in a surface layer with a thickness of 60–100 nm Ag nanoparticles (Ag^0) are present in significant quantities.

To make this result more specific, Fig. 4 shows the depth-dependent Ag modified Auger parameter α', compiled by summation of the Ag $M_4N_{45}N_{45}$ Auger kinetic energy and the Ag $3d_{5/2}$ binding energy, using XE-AES and XPS spectra taken at 60 different depths in the range of 20–200 nm. As static charge corrections cancel in α', it is a more accurate measure for chemical state identification than XE-AES by itself. Reference values of α' for Ag^0 and Ag_2O are indicated by the dashed lines [13]. The gradual change in α' with depth is schematically indicated by the gray band. Fig. 4 shows unambiguously that Ag nanoparticles (Ag^0) are only present in the first 90 ± 20 nm. Additionally, it can be seen that the α' values for the unirradiated sample, as well as for the irradiated sample at larger depths, differ from the Ag_2O literature value, reflecting that the Ag chemical state in $Na^+ \leftrightarrow Ag^+$ ion-exchanged borosilicate glass is different from that of Ag in Ag_2O.

3.3. Refractive index depth profile

Fig. 5 shows optical transmittance (T) and reflectance (R) spectra for samples irradiated with Xe ions at fluences of 1.0×10^{16} (a), 3.0×10^{15} (b), and 5.5×10^{14} (c) ions/cm^2. The transmittance spectra were taken at normal incidence and are corrected for absorption by irradiation-induced defects, by performing a smooth background subtraction [12]. The reflectance spectra were taken at near-normal incidence on the ion-exchanged and ion-irradiated side. All samples show a dip in transmittance at ~2.9 eV (430 nm), corresponding to the surface plasmon resonance energy of spherical Ag nanoparticles embedded in BK7 glass. This dip, which increases in magnitude with ion fluence, is accompanied with a peak in reflectance, being rather broad for the highest ion fluence.

In order to correlate the measured transmittance and reflectance spectra on one hand and the Ag^0 depth profile on the other hand, the spectral transmittance and reflectance were modeled. The calculations are based on the Maxwell–Garnett effective medium theory [17] to convert the Ag^0 depth profile to a refractive index profile, and on the transfer matrix method to subsequently calculate the spectral transmittance and reflectance. In the latter method, the gradually changing refractive index profile was discretized as a series of 1-nm-thick slabs. For every slab, the refractive index was derived from the material composition through the Maxwell–Garnett effective medium theory, which implicitly assumes spherical inclusions (Ag^0 in this case) embedded in a matrix (BK7 glass in this case). The Ag dielectric function was described using literature values [18] whereas the refractive index of the glass was taken to be 1.5. The Ag^0 filling fraction, regarded as being constant for every slab, was considered as the main parameter for determining the complex effective refractive index. The Ag-nanoparticle size was taken into account in the Ag^0 dielectric function through the limited mean free path model for the conduction electrons [1] The particle

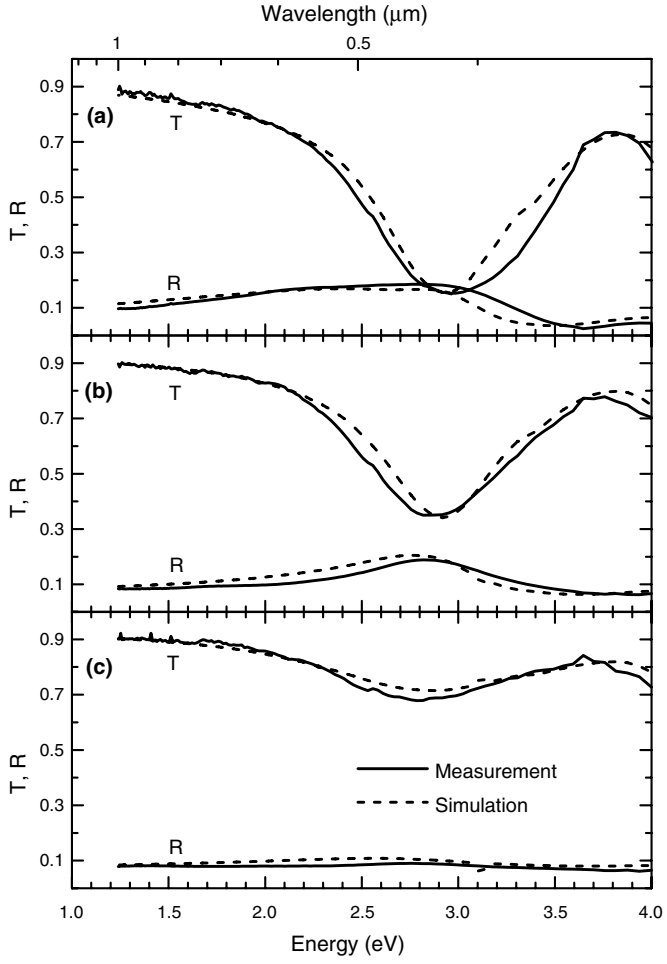

Fig. 5. Optical transmittance (T) and reflectance (R) spectra of 1-MeV-Xe-irradiated $Na^+ \leftrightarrow Ag^+$ ion-exchanged borosilicate glass for (a) 1.0×10^{16}, (b) 3.0×10^{15}, and (c) 5.5×10^{14} ions/cm^2, respectively (solid lines). The dashed lines are the results of simulations based on the transfer matrix method and the Maxwell–Garnett effective medium theory.

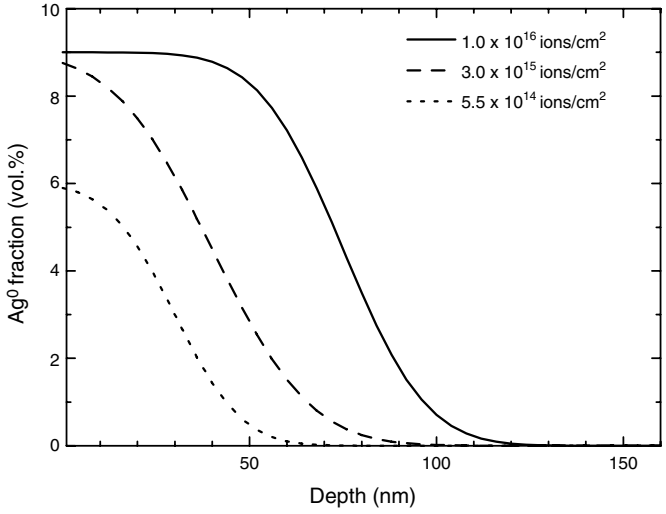

Fig. 6. Ag^0 depth profiles used as inputs for the simulations of the transmittance and reflectance spectra.

size was assumed to be constant with depth for every sample. The depth profile of the Ag^0 volume fraction was described using a complementary error function with three free parameters: surface concentration, characteristic profile thickness, and characteristic profile curvature. The choice for this type of function is motivated by the shape of the Ag^0 depth profile determined from XPS and XE-AES, as shown in Fig. 4.

The simulated transmittance and reflectance spectra, shown as dashed lines in Fig. 5, resemble the measured data quite well. Most features are reproduced, including the low-energy shoulder of the reflection peak for the highest ion fluence (Fig. 5a), which is attributed to interference within the nanocrystal-doped layer. The Ag^0 depth profiles used to obtain these spectra are shown in Fig. 6. The fitted particle diameters are 1.2, 4, and 4 nm for Xe implantation fluences of 5.5×10^{14}, 3.0×10^{15}, and 1.0×10^{16} ions/cm^2, respectively. Given the broad distributions of nanoparticle sizes in each sample, these numbers reflect characteristic values for each sample. The profile for 1.0×10^{16} ions/cm^2 is found to have a maximum Ag^0 content of 9 vol.% [19]. Since the near-surface Ag concentration, as determined by RBS, amounts 10 vol.% (9 at.%), this implies that nearly all Ag is present as nanoparticles (Ag^0). The high simulated Ag^0 surface content is required to account for the relatively strong peak in reflectance, whereas the depth-integrated Ag^0 concentration is largely related to the strength of the transmittance dip. In this way, a unique Ag-nanocrystal depth profile can be found. Small deviations between the data and simulations in Fig. 5 may be due to the fact that the particle diameter varies with depth. According to the Maxwell–Garnett effective medium theory, an Ag-nanocrystal concentration of 9 vol.% corresponds to an effective refractive index of $n = 2.1 + 0.8\,i$ at the resonance wavelength ($\lambda = 430$ nm).

The Ag-nanoparticle depth profile derived from the simulation of the measured transmittance and reflectance spectra for the Xe fluence of 1.0×10^{16} ions/cm^2 is in very good agreement with the depth profile derived from the XPS and XE-AES measurements. This confirms that Ag nucleation mainly occurred in a relatively thin layer below the surface (~80 nm). For the two lower fluences, the simulated Ag^0 content at the surface is lower in order to fit the less pronounced peaks in reflectance, while the total amount of Ag^0 must be lower to account for the smaller dips in transmittance. These constraints lead to the depth profiles shown in Fig. 6 (dashed and dotted lines), with the resulting transmittance and reflectance spectra as shown in Fig. 5(b) and (c).

3.4. Discussion

The conclusion that 1 MeV Xe irradiation of $Na^+ \leftrightarrow Ag^+$ ion-exchanged borosilicate glass induces Ag-nanocrystal nucleation in a layer with a thickness significantly smaller than the corresponding ion range puts a number of earlier published results in a new perspective. First of

all, it implies that the reported effective refractive index of the material used for the fabrication of highly dispersive micropatterns is incorrect [11]. That refractive index was derived under the assumption that the Ag nanocrystals were formed in a layer with a thickness of 450 nm. The corresponding analysis, in which the real and imaginary parts of the effective refractive index were considered as independent variables [20] resulted in peak values of 2.6 for the real and 0.15 for the imaginary parts of the refractive index for a Xe fluence of 5.0×10^{15} ions/cm^2 [11]. From Fig. 6 it can be seen that an irradiation at a Xe fluence of 5.0×10^{15} ions/cm^2 would lead to an Ag-nanocrystal depth profile with a surface content of ~9 vol.%. For such a composition, the effective refractive index is $2.1 + 0.8i$ at the resonance wavelength ($\lambda = 430$ nm), i.e., a significantly lower value for the real part of the refractive index and a much higher value of for the imaginary part compared to Ref. [11]. Consequently, the index contrast of micropatterns fabricated by the described method is lower than originally thought, whereas the extinction is significantly higher. This implies that the material is less attractive for, e.g., the realization of (nonlinear) photonic crystals.

Given the present data, the earlier published analysis that atomic displacement energy loss is the main factor for Ag-nanocrystal nucleation in $Na^+ \leftrightarrow Ag^+$ ion-exchanged glass during ion irradiation must be reconsidered [12]. This analysis was based on a comparison of the energy deposition by electronic excitations and by atomic displacements, both integrated over the full ion range. However, the results presented in this paper indicate that that comparison is not necessarily the most relevant one, as nanocrystals are only formed at depths much smaller than the ion range. To study the Ag-nanocrystal formation mechanism, a more extensive investigation, including the analysis of the nanocrystal depth profiles for irradiations with various species, is required. An example of such an analysis is reported by Valentin et al. [21]. In that paper, the Cu-nanocrystal formation induced by MeV heavy ion irradiation of Cu-containing glass is studied. It is reported that, also in that experiment, nanocrystal formation occurs in a depth range that is much smaller than the range of the ions used to induce the nucleation. Our conclusions are in agreement with those results.

Additionally, this paper provides a new perspective for studies of interaction and sensitizing effects of Ag nanocrystals and optically active Er ions. In a previous paper [22], we demonstrated that Ag ions, incorporated into soda-lime silicate glass by ion-exchange (as in the present paper) act as efficient sensitizer for Er, presumably mediated by a defect state related to Ag ions. It was also noted that no sensitizing effect of Ag nanocrystals on the Er excitation was observed. With the present knowledge that the nanocrystal depth profile is only shallow, and the Er was implanted deeply, it can now be concluded that no such interaction was to be expected in that work. Future work will study the interaction between Ag nanocrystals and Er ions in better overlapping depth profiles in more detail. Near-field effects related to the SPR in the nanoparticles may both enhance the excitation and emission rate of Er ions in glass as has been described theoretically [23], and as has been found experimentally for other types of emitters such as dye molecules [24].

Finally, we note that the Ag-nanoparticle-doped glass studied here has been used as starting material for the fabrication of Ag nanoparticle arrays [25]. In that work, 1-MeV-Xe-irradiated $Na^+ \leftrightarrow Ag^+$ ion-exchanged borosilicate glass was subsequently irradiated with 30 MeV Si ions. The Ag nanoparticle arrays show strong optical anisotropy due to differences in transverse and longitudinal surface plasmon modes in the arrays.

4. Conclusion

By combining multiple techniques (RBS, XPS, XE-AES, and optical transmittance and reflection measurements), we consistently derived the Ag-nanocrystal depth profile as well as the corresponding refractive index profile of 1-MeV-Xe-irradiated $Na^+ \leftrightarrow Ag^+$ ion-exchanged borosilicate glass. It is shown unambiguously that the Ag nanocrystals are formed in a layer with a thickness of 90 ± 20 nm below the surface (for a Xe fluence of 1.0×10^{16} ions/cm^2). The implications of this conclusion for the integration of SPR-based functionalities in photonic devices have been discussed.

Acknowledgements

The authors would like to thank Jan van der Elsken for many useful discussions. This work is part of the research program of the "Stichting voor Fundamenteel Onderzoek der Materie (FOM)", which is financially supported by the "Nederlandse organisatie voor Wetenschappelijk Onderzoek (NWO)".

References

[1] U. Kreibig, M. Vollmer, Optical Properties of Metal Clusters, Springer, Berlin, 1995.
[2] F. Hache, D. Ricard, C. Flytzanis, J. Opt. Soc. Am. B 3 (1986) 1647.
[3] A. Dakka, J. Lafait, C. Sella, S. Berthier, M. Abd-Lefdil, J.-C. Martin, M. Maaza, Appl. Opt. 39 (2000) 2745.
[4] J.W. Haus, N. Kalyaniwalla, R. Inguva, C. Bowden, J. Appl. Phys. 65 (1989) 1420.
[5] G.A. Nikklasson, C.G. Granqvist, J. Appl. Phys. 55 (1984) 3382.
[6] M.J. Bloemer, J.W. Haus, J. Lightwave Tech. 14 (1996) 1534.
[7] G.W. Arnold, J. Borders, J. Appl. Phys. 48 (1977) 1488.
[8] G. De, A. Licciulli, C. Massaro, L. Tapfer, M. Catalano, G. Battaglin, C. Meneghini, P. Mazzoldi, J. Non-Cryst. Solids 194 (1996) 225.
[9] H.B. Liao, R.F. Xiao, J.S. Fu, P. Yu, G.K.L. Wong, P. Sheng, Appl. Phys. Lett. 70 (1997) 1.
[10] F. Caccavale, G. De Marchi, F. Gonella, P. Mazzoldi, G. Meneghini, A. Quaranta, G.W. Arnold, G. Battaglin, G. Mattei, Nucl. Instr. Meth. B 96 (1995) 382.
[11] C. Strohhöfer, J.P. Hoogenboom, A. van Blaaderen, A. Polman, Adv. Mater. 14 (2002) 1815.

[12] D.P. Peters, C. Strohhöfer, M.L. Brongersma, J. van der Elsken, A. Polman, Nucl. Instr. Meth. Phys. Res. B 168 (2000) 237.
[13] C.D. Wagner, W.M. Riggs, L.E. Davis, J.F. Moulder, G.E. Muilenberg, Handbook of X-ray Photoelectron Spectroscopy, Perkin-Elmer, Eden Prairie, MN, 1979.
[14] E. Borsella, E. Cattaruzza, G. De Marchi, F. Gonella, G. Mattei, P. Mazzoldi, A. Quaranta, G. Battaglin, R. Polloni, J. Non-Cryst. Sol. 245 (1999) 122.
[15] G. De Marchi, F. Caccavale, F. Gonella, G. Mattei, P. Mazzoldi, G. Battaglin, A. Quaranta, Appl. Phys. A 63 (1996) 403.
[16] A. Miotello, G. De Marchi, G. Mattei, P. Mazzoldi, Appl. Phys. A 67 (1998) 527.
[17] C.F. Bohren, D.R. Huffman, Absorption and Scattering of Light by Small Particles, Wiley, New York, 1983.
[18] E.D. Palik (Ed.), Handbook of Optical Constants of Solids, Academic, Orlando, FL, 1985.
[19] The Maxwell–Garnett effective medium theory is known to provide reasonably accurate results for the relatively high filling fractions under consideration, see, e.g., A. Liebsch, P.V. González, Phys. Rev. B 29 (1984) 6907.
[20] C. Strohhöfer, Optical properties of ion beam modified waveguide materials doped with erbium and silver, Ph.D. Thesis, Utrecht University, FOM Institute for Atomic and Molecular Physics, Amsterdam, The Netherlands, 2001.
[21] E. Valentin, H. Bernas, C. Ricolleau, F. Creuzet, Phys. Rev. Lett. 86 (2001) 99.
[22] C. Strohhöfer, A. Polman, Appl. Phys. Lett. 81 (2002) 1414.
[23] J. Gersten, A. Nitzan, J. Chem. Phys. 75 (1981) 1139.
[24] A. Wokaun, H.-P. Lutz, A.P. King, U.P. Wild, R.R. Ernst, J. Chem. Phys. 79 (1983) 509.
[25] J.J. Penninkhof, A. Polman, L.A. Sweatlock, S.A. Maier, H.A. Atwater, A.M. Vredenberg, B.J. Kooi, Appl. Phys. Lett. 83 (2003) 4137.